ENHANCED HEAT TRANSFER CHARACTERISTICS OF CONJUGATED AIR JET IMPINGEMENT ON A FINNED HEAT SINK

by

Shuxia QIU[a], Peng XU[a*], Liping GENG[b], Arun S. MUJUMDAR[c], Zhouting JIANG[a], and Jinghua YANG[a]

[a] College of Science, China Jiliang University, Hangzhou, China
[b] College of Metrology and Measurement Engineering, China Jiliang University, Hangzhou, China
[c] Department of Chemical Engineering, Western University, London, Ont., Canada

Original scientific paper
DOI:10.2298/TSCI141229030Q

Air jet impingement is one of the effective cooling techniques employed in micro-electronic industry. To enhance the heat transfer performance, a cooling system with air jet impingement on a finned heat sink is evaluated via the computational fluid dynamics method. A 2-D confined slot air impinging jet on a finned flat plate is modeled. The numerical model is validated by comparison of the computed Nusselt number distribution on the impingement target with published experimental results. The flow characteristics and heat transfer performance of jet impingement on both of smooth and finned heat sinks are compared. It is observed that jet impingement over finned target plate improves the cooling performance significantly. A dimensionless heat transfer enhancement factor is introduced to quantify the effect of jet flow Reynolds number on the finned surface. The effect of rectangular fin dimensions on impingement heat transfer rate is discussed in order to optimize the cooling system. Also, the computed flow and thermal fields of the air impingement system are examined to explore the physical mechanisms for heat transfer enhancement.

Key words: *air jet impingement, finned heat sink, CFD, enhanced heat transfer*

Introduction

With rapidly increasing demand for very compact yet powerful electronic devices, the heat dissipation rate has increased up to tens or even hundreds of W/cm^2. As a result, the main cause of malfunction of electronic devices is reported to be due to overheating. Thus heat dissipation is becoming a major obstacle to further developments in the micro-electronic industries. Various thermal management methods, *e.g.*, heat pipes, micro-channels, jet impingement, spray cooling, solid-state cooling, superlattice and heterostructure cooling, thermionic and thermotunneling cooling, use of phase change materials, *etc.,* have been proposed and developed [1]. Air jet impingement is one of the most common and effective cooling methods due to its high heat transfer rate. Jet impingement heat transfer has been studied extensively in the past, especially for steady jet impingement on a smooth target [2-6]. However, the high heat transfer coefficient of a single jet on the target decays rapidly with distance downstream of impingement surface.

* Corresponding author, e-mail: xupeng@cjlu.edu.cn; pengxuhust@gmail.com

Further enhancement in the convective heat transfer coefficient for jet impingement is to *roughen* the impinging target using fins or extended surfaces. The flow and thermal physics of jets impinging on a rough surface are different from those for a smooth surface. However, it has been reported that rough target plates would reduce the heat transfer from the target plate to the impinging fluid in laminar region [7]. On the other hand for turbulent impinging jets, the heat transfer coefficient can be enhanced significantly for a rough impinging surface [8].

The combination of air jet impingement and finned heat target surface has potential in heat transfer enhancement as the heat sink exhibits smaller thermal resistance over the range of Reynolds number of interest. The effect of *patterned* surface with ribs on heat transfer in impingement systems has been examined by several researchers. They have shown that properly arranged ribs can enhance the heat transfer coefficient for turbulent impinging jet [9-20]. Many researchers have performed experimental studies on various type of air jets (*e.g.*, slot, circular and elliptic jets, *etc.*) impingement on rib-roughened targets. They noted that for a given volume of material, the heat transfer rate can be enhanced significantly by the combination of impingement and finned heat sink [9-12]. Some researchers have investigated the effect of the shape and arrangement of pin-fin sinks (such as triangular, rectangular, orthogonal, V-shaped, inverted V-shaped, convergent-divergent and perforated ribs, *etc.*) on the heat transfer rate in air jet impingement [12-15]. Tan *et al*. [12] have reported that the convective heat transfer rate can be increased up to 30% in the ribbed regions for Reynolds numbers ranging from 6000 to 30000. El-Sheikh and Garimella [13] stated that the heat transfer rates can be increased by a factor of 7.5 to 72 for a range of jet Reynolds numbers from 8000 to 45000. Caliskan and Baskaya [14] and Caliskan [15] reported that the average Nusselt number values for the V-shaped rib-roughened plate can be increased by 4% to 26.6% over those for the smooth plate as the Reynolds number varied from 2000 to 10000, and the perforated rib surface produced higher heat transfer coefficients compared with the smooth and solid rib surfaces.

Recently, numerical simulation has been widely applied in the study of the conjugated cooling system of air jet impingement and finned heat sink; as the numerical predictions are validated by comparison with experimental data, this provides a means to optimize the flow and geometrical parameters. Maveety and Jung [16] validated the numerical method incorporating the k-ε turbulence model by comparison with experiments using an aluminum heat sink subjected to a uniform heat flux using a silicon test chip. Jia *et al*. [17] employed a numerical investigation to determine the velocity and heat transfer characteristics of multiple impinging slot jets in rib-roughened channels in the presence of cross-flow, and discussed the effect size and arrangement of jets and ribs on the heat and mass transfer for jet Reynolds number from 6000 to 14000. Sanyal *et al*. [18] numerically investigated the heat transfer characteristics of confined slot jet impingement on a pin-fin heat sink. Their results indicated that the effective heat transfer coefficient increases with fin height for the steady jet impingement on a pin-fin heat sink. Xing *et al*. [19] presented experimental and numerical results on heat transfer characteristics of jet arrays impinging on micro-rib roughened surfaces. They have shown that the overall heat transfer performance on the micro-rib roughened plate is always best for minimum cross-flow case, and that the heat transfer enhancement ratio increases with increasing Reynolds numbers. Spring *et al*. [20] found that the ribbed impinging surfaces show no improvement in Nusselt number for the in-line jet pattern but alleviate the strong degrading effect of cross-flow in the downstream zone for the staggered jet arrangement. Huang *et al*. [21] presented a 3-D simulation for an impingement heat sink module with a commercial code and Levenberg-Marquardt method. They optimized the non-uniform fin width via minimizing the thermal resistance and found that the thermal performance of the optimal heat sink can be improved significantly.

However, the related fluid and thermal physics for jet impingement on a fined heat sink are not yet well-understood due to the complexity of flow structures and non-linear dynamics in the boundary layer. Also, the heat transfer performance of the conjugated system is strongly dependent on the geometry and dimension of impinging jet and heat sink as well as the fluid and thermal conditions. Therefore, this work aims to examine the effect of finned heat sink on the heat transfer in the air jet impingement via numerical simulation. A 2-D slot jet impinging on a fined heat sink is modeled using the CFD method. The effect of jet Reynolds number and geometrical configuration are discussed for further understanding of flow and thermal characteristics.

Mathematical model

A schematic representation of semi-confined jet impingement on a finned heat sink is shown in fig. 1. The base plate is subjected to a uniform constant heat flux. The cooling medium discharged from a slot nozzle of width, W, impinges normally onto a finned heat sink. The nozzle-to-plate distance is H, and the length of the impingement system is L. The rectangular fin is fixed on the base of heat sink located on the central of jet nozzle, the fin width and height are d and h, respectively. As the length of the slot nozzle and the fin are the same, the present flow can be simplified to 2-D problem. In order to examine the effect of finned target surface on the heat transfer properties, the dimensionless impinging height, length, and base thickness are fixed at $H/W = 4$, $L/W = 8$, and $s/W = 0.4$, respectively.

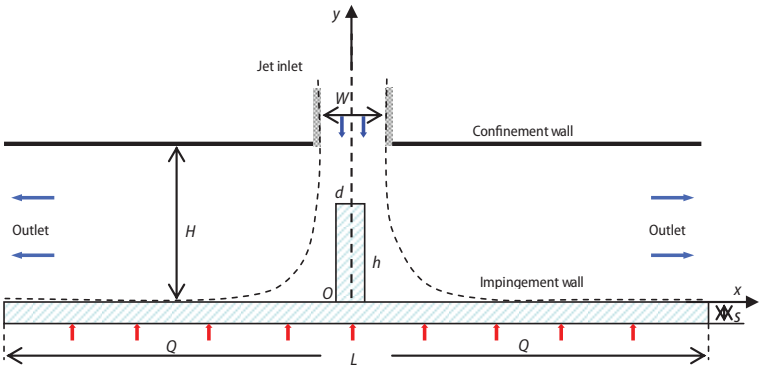

Figure 1. Schematic diagram of the 2-D confined slot jet impingement on a fined heat sink

Considering that only the fin geometry is changed, the governing equations and boundary conditions remain unchanged from geometry to geometry. The cooling medium (air) was assumed to be incompressible with constant physical properties. The finned heat sink is made of aluminum. Based on these assumptions, flow heat transfer within the computational domain is determined by the equations for conservation of mass, momentum, and energy in the Cartesian co-ordinate system:

$$\frac{\partial u_i}{\partial x_i} = 0 \tag{1}$$

$$\frac{\partial(\rho u_i)}{\partial t} + \frac{\partial(\rho u_i u_j)}{\partial x_j} = -\frac{\partial p}{\partial x_i} + \frac{\partial}{\partial x_j}\left[\mu\left(\frac{\partial u_i}{\partial x_j} + \frac{\partial u_j}{\partial x_i}\right) - \rho\overline{u_i' u_j'}\right] + \rho g_i \tag{2}$$

$$\rho c_p \left[\frac{\partial T}{\partial t} + \frac{\partial (u_i T)}{\partial x_i} \right] = \frac{\partial}{\partial u} \left(k \frac{\partial T}{\partial x_i} - \rho c_p \overline{u_i' T'} \right) \tag{3}$$

where u is the velocity component, p – the pressure, ρ – the fluid density, μ represents dynamic viscosity, k – the thermal conductivity, c_p – the specific heat capacity, t and T are time and temperature, respectively. The confinement wall of the jet impingement and bilateral walls of the base plate were considered to be adiabatic. The constant heat flux, applied to the target surface is Q = 1000 W/m^2. A no-slip boundary condition was applied on all solid walls. Uniform velocity, temperature, turbulent kinetic energy, and energy dissipation rate profiles were assumed at the nozzle exit, while the pressure outlet boundary condition was applied at outlet planes. The Reynolds number based on jet exit velocity u_{jet} and slot width, W, is defined as Re = $\rho u_{\text{jet}} W/\mu$. The jet inlet and atmospheric temperature were kept constant at $T_{\text{jet}} = T_\infty$ = 300 K. The physical properties and boundary conditions are shown in tab. 1.

Table 1. Physical properties and system data

Properties/system data	Values
Air density, ρ	1.225 kg/m^3
Air dynamic viscosity, μ	1.7894·10^{-5} kg/ms
Air thermal conductivity, k	0.0242 W/mK
Aluminum thermal conductivity, K	202.4 W/mK
Air specific heat, c_p	1006.43 J/kgK
Atmospheric temperature, T_∞	300 K
Temperature of jet flow, T_{jet}	300 K
Heat flux, Q	1000 W/m^2
Impinging height, H/W	4
Impinging length, L/W	8
Base thickness, s/W	0.4
Jet exit velocity, u_{jet}	10~50 m/s
Jet Reynolds number, Re	3,420~17,120
Fin width, d/W	0.2~0.8
Fin height, h/W	0.4~2.0

The flow and thermal fields was computed with the finite volume CFD code FLUENT. Comparing with standard k-ε model, the renormalization group (RNG) k-ε model includes additional terms for dissipation rate ε development which can significantly improve the accuracy for rapidly strained flows [22]. Therefore, the RNG k-ε turbulence model is numerically robust and fast, and has been proven to be effective in modeling this type of complex flows in impinging and opposed jets [23, 24].

The steady-state simulation was employed, and the initial conditions (t = 0) throughout the computational domain are described as: $u_i = u_j = 0$, $p = p_\infty$, $T = T_\infty$. As the initial values of the turbulent kinetic energy and dissipation rate show marginal effect on the heat transfer, the default initial values were used here. A second upwind discretization scheme was used considering the stability of solution convergence and the SIMPLEC algorithm was employed for the pressure-velocity coupling. A non-uniform grid structure was used with fine meshing near the impingement region and the heat sink, and a coarser mesh away from it. Grid independence of the final results has been checked by analysis of Nusselt number distribution for different grid densities. The solution was considered converged when the normalized energy residual was less than 10^{-6} and the normalized residuals of all the other variables were less than 10^{-4}.

Results and discussion

There are several parameters that affect the thermal performance of the jet impingement system. In the present study, the effects of Reynolds number and the fin on the heat transfer rate are investigated. The local Nusselt number for the impingement surface can be:

$$\text{Nu} = \frac{q''}{T_\text{w} - T_j} \frac{W}{k} \tag{4}$$

The thermal conductivity of jet fluid k can be calculated at jet temperature T_{jet} [25]. A dimensionless factor ε_H is defined as the ratio of the averaged Nusselt number of the finned rough surface $\overline{\mathrm{Nu}}_r$ to that of smooth surface $\overline{\mathrm{Nu}}_s$:

$$\varepsilon_H = \frac{\overline{\mathrm{Nu}}_r}{\overline{\mathrm{Nu}}_s} \tag{5}$$

In order to validate the present numerical model, the Nusselt number under the conditions Re = 6000, Q = 8000 W/m^2, H/W = 1, and the uniform fin dimensions ($d/W = h/W$ = 0.5) was compared with the experimental results of Tan *et al*. [12]. The coolant air was discharged through the orifice plate to impinge on a 1.5 mm Cu plate, and the spent air was constrained inside a semi-confined channel. According to the experimental results, the ambient temperature was taken as 10 ºC and the main heat loss due to natural convection and radiation is 12 W/m^{2}K. It can be seen from the comparison in fig. 2 that the agreement between the present numerical predictions and experimental data is acceptable. The difference of local Nusselt number around the rib can be attributed to the 8% experimental uncertainty and experimental methodology. In the experiment of Tan *et al.* [12], the convective heat transfer was evaluated by the thermal image recorded by the infrared camera and averaged Nusselt number was calculated accordingly.

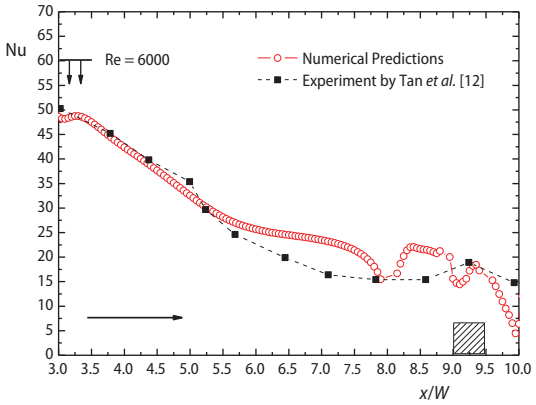

Figure 2. The Nusselt number distribution along the impingement target under jet Re = 6000

For the jet impingement on a smooth surface, the jet issued from the nozzle spreads as a free jet and reaches the stagnation region. And then the flow proceeds as wall-jets on the sides and decelerates in the flow direction while the boundary layer thickness increases monotonically. It can be seen in fig. 3(a) that the local Nusselt number increases slightly from the stagnation point and then decreases along the target plate with the increase of thermal boundary layer thickness. The secondary peaks in the Nusselt number increase in magnitude and shift away from the stagnation point, which can be ascribed to the shift of the secondary re-circulation zone at higher Reynolds numbers. This phenomenon has been reported and discussed by both of experimental and numerical researches [26, 27]. It is observed that the local Nusselt number increases as jet Reynolds number increases from 3420 to 17120, but the enhancement extent decreases from 43% to 9%. Also, the effect of stagnation region increases with increased jet Reynolds number. Figure 3(b) shows that the temperature of the heat sink surface can be lowered by increased jet Reynolds number, however, this effect is margined for high Reynolds numbers. Therefore, it is not practical to enhance the heat transfer rate by increasing only the jet Reynolds number.

Figures 4(a) and 4(b) show the contours of pressure and velocity magnitude for the case of jet impingement on a heat sink with fin width and height of d/W = 0.4 and h/W = 2 at Re = 3420 and H/W = 4. It can be seen that the flow pattern is different from that for the smooth surface case. As the rectangular fin is located at the center of the jet nozzle, a small stagnation region is formed on the top surface of the fin. And two symmetrical flow regions of low velocity are found on both sides of the fin. However, the heat transfer rate around the fin is not reduced

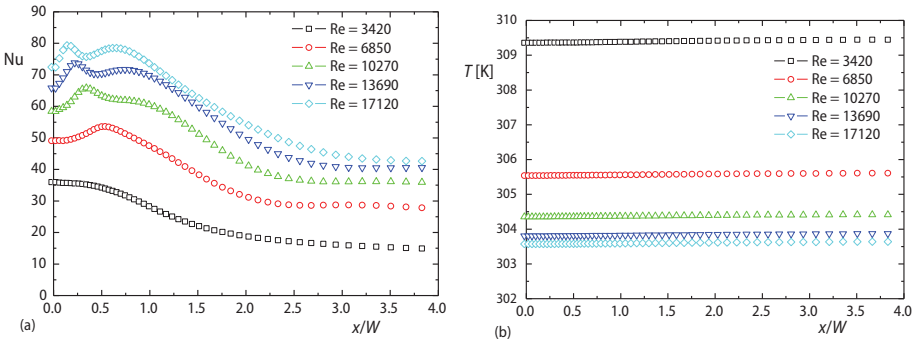

Figure 3. Effect of jet Reynolds number on: (a) local Nusselt number distribution and (b) temperature distribution along the smooth impinging target for $H/W = 4$

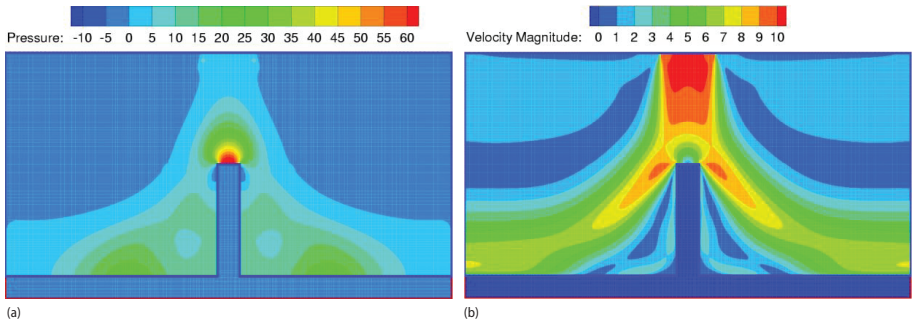

Figure 4. The contours of pressure (a) and velocity magnitude (b) for the jet impingement on a finned heat sink under $H/W = 4$, $L/W = 8$, $d/W = 0.4$, $h/W = 2$, and Re = 3420
(*for color image see journal web site*)

as the fin extends the heat transfer area. Figure 5 shows the computed surface temperature distribution along the target for single jet impingement on a smooth target and conjugated air jet impingement with a single finned heat sink at the same Re = 3420. Applying a single fin with $d/W = 0.4$ and $h/W = 2$, the Nusselt number can be increased up to 50% and the impingement target surface temperature can be lowered about 2 K. Thus, the conjugated system reduces the

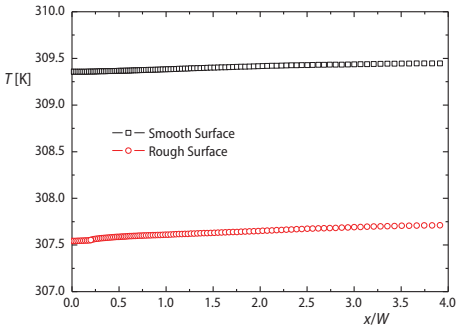

Figure 5. Temperature distribution along the smooth and finned rough surfaces ($d/W = 0.4$ and $h/W = 2$) under Re = 3420 and $H/W = 4$

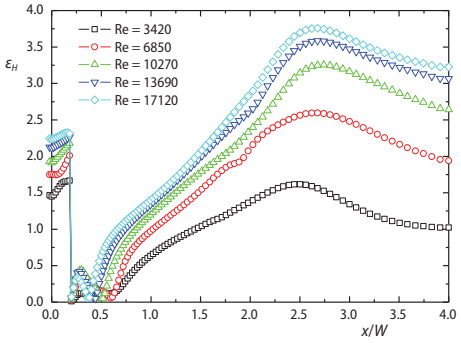

Figure 6. Effect of jet Reynolds number on the enhancement factor for finned target surface at $d/W = 0.4$ and $h/W = 2$

surface temperature of the impinging wall and improves the cooling performance compared with jet impingement on a smooth target.

Figure 6 shows the effect of jet flow Reynolds number on the enhancement factor ε_H for the finned rough surface with $d/W = 0.4$ and $h/W = 2$. Similar to the case of a smooth surface, the Nusselt number can be increased by enhancing the jet flow Reynolds number. It can be seen in fig. 6 that the value of ε_H is greater than 1.0 except for the stagnation region around both sides of the fin. This means that the finned surface can significantly enhance the local heat transfer rate in the wall jet region of the target but does lower it in the stagnation region. It can be also seen in fig. 6, that the value of the dimensionless factor ε_H can be increased by increasing the Reynolds number, however, the amplification will decrease as the jet flow Reynolds number increases.

The width and height of the fin indicate significant effect on the heat transfer of the jet impingement on the finned heat sink. Figures 7(a) and 7(b), respectively, show the effect of fin width on the Nusselt number and temperature distributions along the base of the heat sink. With increased fin width and fixed height, the heat transfer area is clearly increased. However, the fin with increased width will block the cool jet flow impinging the base target and thus reduce the convective heat transfer around both sides of the fin. It can be seen from fig. 7(a) that the local Nusselt number along the top wall of the fin is much higher than that along the base wall. The local Nusselt number along the top wall of the fin is highest at $d/W = 0.4$, but the local Nusselt number on the both sides of the fin is reduced with increased fin width. From fig. 7(b), it can be seen that the base temperature is lowered as the fin width increases from $d/W = 0.2$ to $d/W = 0.4$. However, the base temperature increases with further increase of the fin width. It can be concluded from these results that the base temperature for $d/W = 0.4$ is the lowest and most uniform; this means the fin with width of $d/W = 0.4$ performs best under the current conditions examined ($H/W = 4$, $h/W = 2$, and Re = 3420).

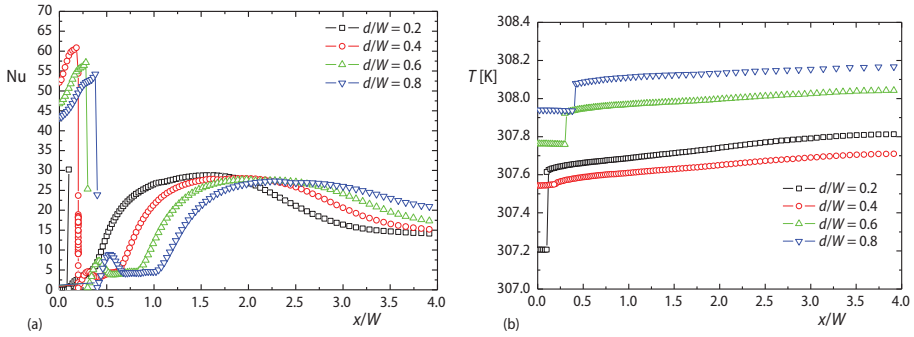

Figure 7. Effect of fin width on the local Nusselt number (a) and temperature (b) distributions along the impinging target at $h/W = 2$ and $Re = 3420$

In order to examine the effect of fin height on the heat transfer properties, the fin width is fixed at $d/W = 0.4$ while its height is varied. Figure 8 shows the effect of h/W from 0.4 to 2.0 on the heat transfer rate. Increased fin height can simultaneously extend heat transfer area and affect the flow pattern and the convective heat transfer rate. The local Nusselt number along the top surface of the fin increases and that of the base surface beside the fin decrease with increased fin height in fig. 8(a). From fig. 8(b), it can be seen that the temperature of the impinging target is lowered as the fin height increases from $h/W = 0.4$ to $h/W = 0.8$ and $h/W = 1.2$, and increases as the fin height increases from $h/W = 1.2$ to 1.6, but then the temperature can be lowered again as the fin height reaches to 2.0. From fig. 8(b), the optimal value is

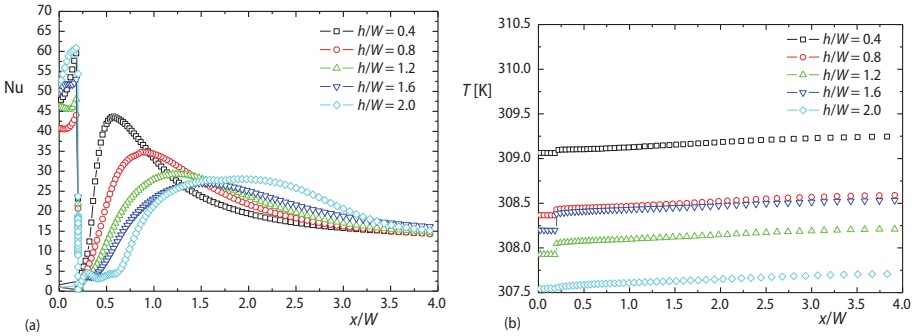

Figure 8. Effect of fin height on the local Nusselt number (a) and temperature (b) distributions along the impinging target $d/W = 0.4$ and Re = 3420

$h/W = 2$ from the heat transfer point of view. This is true for the geometric, flow and material values used in the model.

Concluding remarks

In the current work, a mathematical modeling has been developed for a 2-D confined slot air jet impingement. The flow and thermal physics of the air jet impingement on a finned heat sink are significantly different from that of smooth surface, and the rough finned heat sink can enhance the heat transfer rate of the air jet impingement. The numerical results indicate that the jet Reynolds number and fin dimension can evidently affect the heat transfer performance. Increased fin width and height can simultaneously extend heat transfer area and affect the convective heat transfer for the impinging jet. For a typical case at $H/W = 4$, $L/W = 8$, and Re = 3420, the optimized fin width and height are $d/W = 0.4$ and $h/W = 2$, and the Nusselt number for the finned target surface can be increased up to 50% compared with that of smooth surface. With the current mathematical model, the fin arrangement of the conjugated cooling system can be simulated and optimized accordingly.

Acknowledgement

This work was supported by the National Natural Science Foundation of China through Grant No. 11202201, 51206153, and 21204078, Zhejiang Provincial Natural Science Foundation of China through Grant No. LQ16E060002 and LY16A020002.

Nomenclature

c_p – air specific heat, [Jkg^{-1}K^{-1}]
d – fin width, [m]
g – gravity acceleration [ms^{-2}]
H – nozzle-to-plate spacing, [m]
h – fin height, [m]
K – solid thermal conductivity, [Wm^{-1}K^{-1}]
k – air thermal conductivity, [Wm^{-1}K^{-1}]
L – jet length, [m]
Nu – Nusselt number, eq. (4), [–]
$\overline{\text{Nu}}$ – averaged Nusselt number, [–]
p – static pressure, [Pa]
Q – heat transfer rate, [Wm^{-2}]
q'' – heat flux, [Wm^{-2}]
Re – Reynolds number (= $\rho u_{jet} W/\mu$), [–]
s – base thickness, [m]
T – temperature, [K]
t – time, [s]
u – velocity, [ms^{-1}]
W – slot width, [m]
x, y – Cartesian co-ordinates, [m]

Greek symbols

ε_H – heat transfer enhancement factor, eq. (5), [–]
μ – dynamic viscosity, [kgm^{-1}s^{-1}]
ρ – density, [kgm^{-3}]

Subscripts

′ – fluctuation
i, *j* – indices in Einstein summation convention
j – jet flow
jet – jet inlet
r – rough target surface
s – smooth target surface
w – impingement wall
∞ – atmospheric

References

[1] Lasance, C., Simons, R. E., Advances in High-Performance Cooling for Electronics, *Electronics Cooling*, *11* (2005), Nov., p. 24
[2] Lienhard, V. J. H., Liquid Jet Impingement, in: *Annual Review of Heat Transfer* (Ed. C. L. Tien), Begell Hourse, N. Y., USA, 1995, pp. 199-270
[3] Mujumdar, A. S., Impingement Drying, in: *Handbook of Industrial Drying* (Ed. A. S. Mujumdar), Taylor & Francis Group, N. Y., USA, 2007, pp. 385-395
[4] Al-Hadhrami, L., *et al*.**,** Heat Transfer in a Channel with Inclined Target Surface Cooled by Single Array of Impinging Jets, *Proceedings,* ASME Turbo Expo, Montreal, Canada, 2007, Vol. 4A, pp. 35-42
[5] Al-Mubarak, A. A., *et al*.**,** Impact of Jet Reynolds Number and Feed Channel Geometry on Heat Transfer in a Channel with Inclined Target Surface Cooled by Single Array of Centered Impinging Jets with Outflow in Both Directions, *Proceedings*, World Congress on Engineering, London, UK., 2011,Vol. III, p. 1495
[6] Al-Mubarak, A. A., *et al*., Heat Transfer in a Channel with Inclined Target Surface Cooled by Single Array of Centered Impinging Jets, *Thermal Science, 17* (2013), 4, pp.1195-1206
[7] Lou, Z. W., *et al*., Effects of Geometric Parameters on Confined Impinging Jet Heat Transfer, *Applied Thermal Engineering, 25* (2005), 17-18, pp. 2687-2697
[8] Sagot, B., *et al*., Enhancement of Jet-to-Wall Heat Transfer Using Axisymmetric Grooved Impinging Plates, *International Journal of Thermal Sciences, 49* (2010), 6, pp. 1026-1030
[9] Gau, C., Lee, I. C., Flow and Impingement Cooling Heat Transfer along Triangular Rib-Roughened Walls, *International Journal of Heat and Mass Transfer, 43* (2000), 24, pp. 4405-4418
[10] Yan, W., Mei, S., Measurement of Detailed Heat Transfer along Rib-Roughened Surface under Arrays of Impinging Elliptic Jets, *International Journal of Heat and Mass Transfer, 49* (2006), 1-2, pp. 159-170
[11] Katti, V., Prabhu, S. V., Heat Transfer Enhancement on a Flat Surface with Axisymmetric Detached Ribs by Normal Impingement of Circular Air Jet, *International Journal of Heat and Fluid Flow, 29* (2008), 5, pp. 1279-1294
[12] Tan, L., *et al*., Jet Impingement on a Rib-Roughened Wall Inside Semi-Confined Channel, *International Journal of Thermal Sciences, 86* (2014), Dec., pp. 210-218
[13] El-Sheikh, H. A., Garimella, S. V., Enhancement of Air Jet Impingement Heat Transfer Using Pin-Fin Heat Sinks, *IEEE Transactions on Components and Packaging Technology, 23* (2000), 2, pp. 300-308
[14] Caliskan, S., Baskaya, S., Experimental Investigation of Impinging Jet Array Heat Transfer from a Surface with V-Shaped and Convergent-Divergent Ribs, *International Journal of Thermal Sciences, 59* (2012), Sep., pp. 234-246
[15] Caliskan, S., Flow and Heat Transfer Characteristics of Transverse Perforated Ribs under Impingement Jets, *International Journal of Heat and Mass Transfer, 66* (2013), Nov., pp. 244-260
[16] Maveety, J. G., Jung, H. H., Design of an Optimal Pin-Fin Heat Sink with Air Impingement Cooling, *International Communications in Heat and Mass Transfer, 27* (2000), 2, pp. 229-240
[17] Jia, R., *et al*., Impingement Cooling in a Rib-Roughened Channel with Cross-Flow, *International Journal of Numerical Methods for Heat & Fluid Flow, 11* (2001), 7, pp. 642-662
[18] Sanyal, A., *et al*., Numerical Study of Heat Transfer from Pin-Fin Heat Sink Using Steady and Pulsated Impinging Jets, *IEEE Transactions on Components and Packing Technology, 32* (2009), 4, pp. 859-867
[19] Xing, Y., *et al*., Experimental and Numerical Investigation of Impingement Heat Transfer on a Flat and Micro-Rib Roughened Plate with Different Cross Flow Schemes, *International Journal of Thermal Sciences, 50* (2011), 7, pp. 1293-1307
[20] Spring, S., *et al*., An Experimental and Numerical Study of Heat Transfer from Arrays of Impinging Jets with Surface Ribs, *ASME Journal of Heat Transfer, 134* (2012), 8, pp. 082201-082211
[21] Huang, C.-H., *et al*. An Impingement Heat Sink Module Design Problem in Determining Optimal Non-Uniform Fin Widths, *International Journal of Heat and Mass Transfer, 67* (2013), Dec., pp. 992-1006
[22] Yakhot, A., Ozag, S. A., Renormalization Group Analysis of Turbulence: I. Basic Theory, *Journal of Scientific Computing, 1* (1986), 1, pp. 1-51

[23] Sharif, M. A. R., Mothe, K. K., Parametric Study of Turbulent Slot-Jet Impingement Heat Transfer from Concave Cylindrical Surfaces, *International Journal of Thermal Science, 49* (2009), 2, pp. 428-442
[24] Parham, K., *et al*., A Numerical Study of Turbulent Opposed Impinging Jets Issuing from Triangular Nozzles with Different Geometries, *Heat and Mass Transfer, 47* (2011), 4, pp. 427-437
[25] Xu, P., *et al*., Heat Transfer under a Pulsed Slot Turbulent Impinging Jet at Large Temperature Differences, *Thermal Science, 14* (2010), 1, pp. 271-281
[26] Garimella, S. V., Heat Transfer and Flow Fields in Confined Jet Impingement, *Annual Review of Heat Transfer, 11* (2000), pp. 413-494
[27] Katti, V., Prabhu, S. V., Experimental Study and Theoretical Analysis of Local Heat Transfer Distribution between Smooth Flat Surface and Impinging Air Jet from a Circular Straight Pipe Nozzle, *International Journal of Heat and Mass Transfer, 51* (2008), 17-18, pp. 4480-4495

Paper submitted: December 29, 2014
Paper revised: February 5, 2015
Paper accepted: February 11, 2015